Introduction to Control and Robotic Systems
Antenna Angular Position Control System Design Project
EE 386 - 01

Sean Mitchell

Submitted April 18th, 2018

Instructor: Dr. Yuri Shtessel

1 Introduction

The main objective of this project was to derive a way to stabilize the angular position of a rotating antenna. The problem of stabilizing a rotating antenna is important because antennas need to be accurately positioned to properly receive a signal of interest. An uncontrolled, moving antenna will make it difficult, if not impossible to track the signal of interest.

Two possible controllers were derived to solve this problem. The first was a Proportional + Derivative, or PD, controller. The second was a Proportional + Integral + Derivative, or PID, controller. Both of these controllers utilized prefilters to simplify the design process. Stability of both control systems was verified using the Routh-Hurwitz criterion, Nyquist criterion, and Bode plots.

2 Controller Design

2.1 PD Controller Design

Beginning with the transfer function derived from Fig 2, while neglecting the dynamics of the armature winding, L_a.

$$\frac{\Omega_m}{V_a} = \frac{[\frac{K_m}{R_a} - NT_d][\frac{1}{Js+f}]}{1 + [\frac{K_m}{R_a} - NT_d][\frac{1}{Js+f}]K_b} \tag{1}$$

Simplifying equation 1

$$\frac{\Omega_m}{V_a} = \frac{0.6 - 0.1T_d}{0.05s + 0.1 + (0.6 - 0.1T_d)0.6} \tag{2}$$

Next, the PD controller, $G_c(s)$, and the $K_\theta sensor$ feedback loop are added. The disturbance, T_d, is also set to zero here.

$$\frac{0.6(K_P + K_D s)0.1}{5(0.05s + 0.1 + 0.36) + 0.6(K_P + K_D s)(0.1)(K_\theta sensor)} \tag{3}$$

$$\frac{0.6(K_P + K_D s)0.1}{0.5s^2 + 4.6s + 0.6(K_P + K_D s)(0.1)(K_\theta sensor)} \tag{4}$$

$$\frac{1.2K_P + 1.2K_D s}{s^2 + (9.2 + 1.2K_D)s + 1.2K_P} \tag{5}$$

Next, the gain values K_P and K_D are found. For these computations, the values of $T_s = 1.2s$ and percent overshoot = 12 were used.

$$K_P = 2\zeta\omega_n$$

$$K_D = \omega_n^2$$

$$\zeta\omega_n = \frac{12}{1.2} = 10$$

Therefore

$$K_P = 20$$

$$K_D = 200$$

Substituting the gain values into equation 5

$$\frac{1.2(20)s + 1.2(200)}{s^2 + (9.2 + 1.2(20))s + 1.2(200)} \tag{6}$$

$$\frac{24s + 240}{s^2 + 249s + 240} \tag{7}$$

$$\frac{24(s + 10)}{s^2 + 249s + 240} \tag{8}$$

Applying the prefilter, $G_{pf}(s)$

$$\frac{24(s + 10)G_{pf}(s)}{s^2 + 249s + 240}, G_{pf}(s) = \frac{10}{s + 10} \tag{9}$$

Finally, the transfer function of the PD controller is

$$\frac{240}{s^2 + 249s + 240} \tag{10}$$

The steady state error e_{ss_θ} of equation 10 is

$$\lim_{s \to 0} s(\frac{240}{s^2 + 249s + 240})(\frac{1}{s}) = 1 \tag{11}$$

Rewriting equation 1 so that $R(s) = 0$, the transfer function of the disturbance, T_d is

$$\frac{N}{s(Js + f) + (K_m K_B s - N(K_P + K_D s)} \tag{12}$$

The steady state error $e_{ss_{T_d}}$ of equation 12 is

$$\lim_{s \to 0} s(\frac{N}{s(Js + f) + (K_m K_B s - N(K_P + K_D s)})(\frac{12}{s}) = 0.06 \tag{13}$$

2.2 PID Controller Design

the transfer function derived from Fig 2, while neglecting the dynamics of the armature winding, L_a.

$$\frac{\Omega_m}{V_a} = \frac{[\frac{K_m}{R_a} - NT_d][\frac{1}{Js+f}]}{1 + [\frac{K_m}{R_a} - NT_d][\frac{1}{Js+f}]K_b} \tag{14}$$

Simplifying equation 1

$$\frac{\Omega_m}{V_a} = \frac{0.6 - 0.1T_d}{0.05s + 0.1 + (0.6 - 0.1T_d)0.6} \tag{15}$$

Next, the PID controller, $G_c(s)$, and the $K_\theta sensor$ feedback loop are added. The disturbance, T_d, is also set to zero here.

$$\frac{0.6(K_P + K_D s + \frac{K_I}{s})0.1}{5(0.05s + 0.1 + 0.36) + 0.6(K_P + K_D s + \frac{K_I}{s})(0.1)(K_\theta sensor)} \tag{16}$$

$$\frac{1.2K_P + 1.2K_D s}{s^2 + (9.2 + 1.2K_D)s + 1.2K_P} \tag{17}$$

$$\frac{1.2K_D s^2 + 1.2K_I s + 1.2K_P}{s^3 + (9.2 + 1.2K_D)s^2 + 1.2K_P s + 1.2K_I} \tag{18}$$

Using the ITAE criterion [1], the gains K_D, K_I, and K_P were computed.

$$1.75\omega_n = 9.2 + 1.75K_D$$

$$2.15\omega_n^2 = 1.2K_P$$

$$\omega_n^3 = 1.25K_I$$

Solving for K_D, K_I, and K_P

$$K_D = 41.96$$

$$K_I = 124.32$$

$$K_P = 481.67$$

Substituting these three gain values into equation 18

$$\frac{1.2(41.96)s^2 + 1.2(124.32)s + 1.2(481.67)}{s^3 + (9.2 + 1.2(41.96))s^2 + 1.2(481.67)s + 1.2(124.32)} \tag{19}$$

$$\frac{50.357s^2 + 149.184s + 578.004}{s^3 + 59.552s^2 + 149.184s + 578.004} \tag{20}$$

$$\frac{50.357s^2 + 149.184s + 578.004}{s^3 + 59.552s^2 + 149.184s + 578.004} \tag{21}$$

Applying the prefilter, $G_{pf}(s)$

$$\frac{(50.357s^2 + 149.184s + 578.004)G_{pf}(s)}{s^3 + 59.552s^2 + 149.184s + 578.004}, G_{pf}(s) = \frac{11.48}{s^2 + 2.96s + 11.48} \tag{22}$$

Finally, the transfer function of the PID controller is

$$\frac{578.004}{s^3 + 59.552s^2 + 149.184s + 578.004} \tag{23}$$

The steady state error e_{ss_θ} of equation 23 is

$$\lim_{s\to 0} s(\frac{578.004}{s^3 + 59.552s^2 + 149.184s + 578.004})(\frac{1}{s}) = 1 \tag{24}$$

Rewriting equation 14 so that $R(s) = 0$, the transfer function of the disturbance, T_d is

$$\frac{N}{S(Js + f) + K_M K_B s^2 + N(K_P + K_D s + K_I)} \tag{25}$$

The steady state error $e_{ss_{T_d}}$ of equation 25 is

$$\lim_{s\to 0} s(\frac{N}{S(Js + f) + K_M K_B s^2 + N(K_P + K_D s + K_I)})(\frac{12}{s}) = 0.02 \tag{26}$$

3 Stability Analysis

3.1 PD Stability Analysis

Starting with the transfer function of the PD controller

$$\frac{240}{s^2 + 249s + 240} \tag{27}$$

$$q(s) = s^2 + 249s + 2404 \tag{28}$$

The Routh-Hurwitz criterion of stability is

$$\begin{array}{c|cc} s^3 & 1 & 240 \\ s^2 & 249 & 0 \\ s^1 & b_1 & 0 \end{array}$$

$$b_1 = \frac{(-1)(249)(-249 * 240}{=} 240$$

$$\begin{array}{c|cc} s^3 & 1 & 240 \\ s^2 & 249 & 0 \\ s^1 & 240 & 0 \end{array}$$

There are no sign changes on the right column, therefore the system is stable.

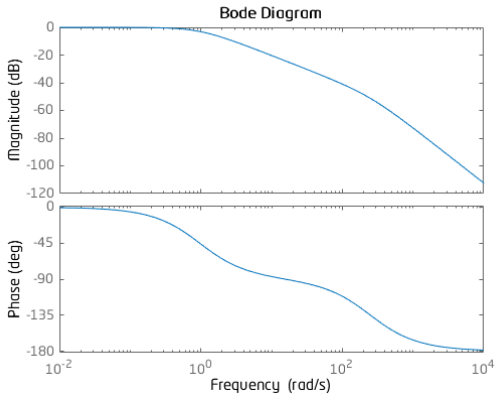

Figure 1: Bode plot of equation 10

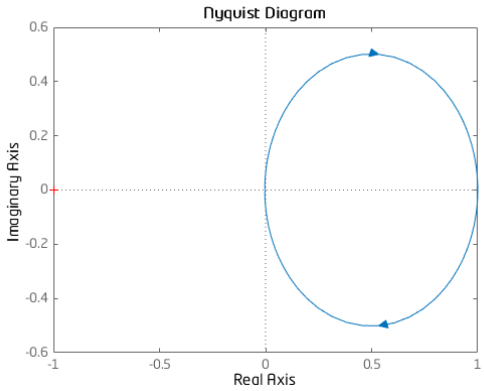

Figure 2: Nyquist plot of equation 10

3.2 PID Stability Analysis

Starting with the transfer function of the PID controller

$$\frac{578.004}{s^3 + 59.552s^2 + 149.184s + 578.004} \tag{29}$$

$$q(s) = s^3 + 59.552s^2 + 149.184s + 578.004 \tag{30}$$

The Routh-Hurwitz criterion of stability is

s^3	1	149.18
s^2	59.552	578.004
s^1	b_1	0
s^0	c_1	0

$$b_1 = \frac{(59.552)(1) - (577.004)(149.18)}{59.552} = 139.47$$

$$c_1 \frac{b_1 * 578.004}{b_1} = 578.004$$

s^3	1	149.18
s^2	59.552	578.004
s^1	139.47	0
s^0	578.004	0

There are no sign changes on the right column, therefore the system is stable.

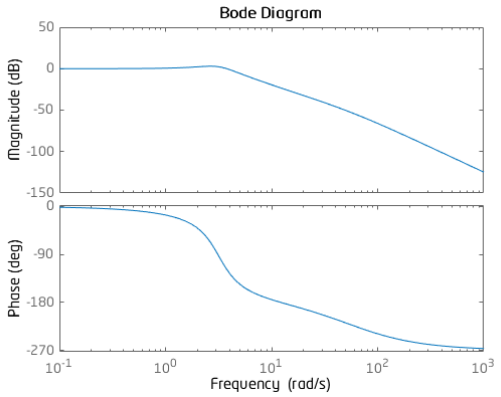

Figure 3: Bode plot of equation 23

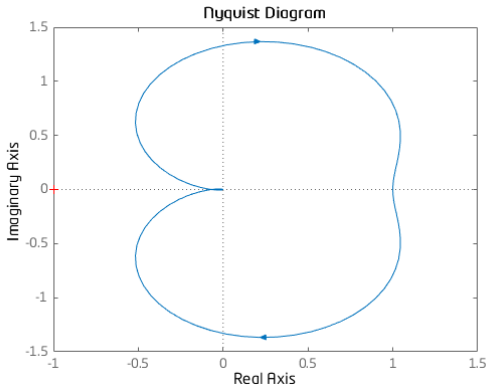

Figure 4: Nyquist plot of equation 23

4 Simulations

Using the previously derived transfer functions and MATLAB, the two controllers were simulated. Using this information and tools, four simulations were performed. The first simulation performed was of the PD controller with no prefilter. The second simulation was a PD controller with a prefilter. The third simulation was the same PD controller with no prefilter. The final simulation was a PID controller with a prefilter.

4.1 Simulation of PD Controller

The following five plots show the simulation of the PD controller. From these plots, it is clear the PD controller is able to successfully stabilize the angular position, θ_A, after the disturbance occurs, but the controller is not able to return it to the desired value.

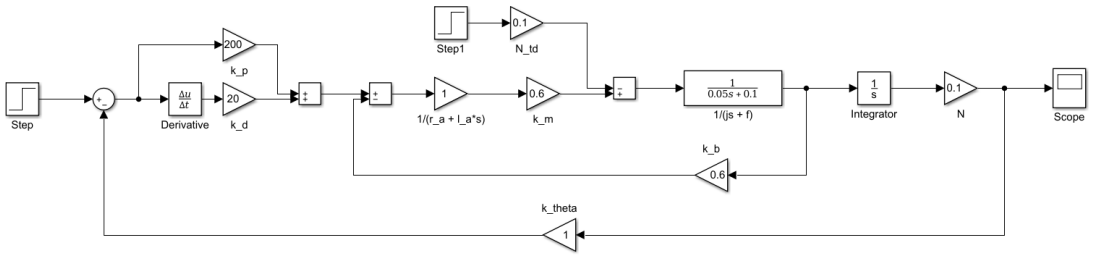

Figure 5: Block diagram of the PD controller

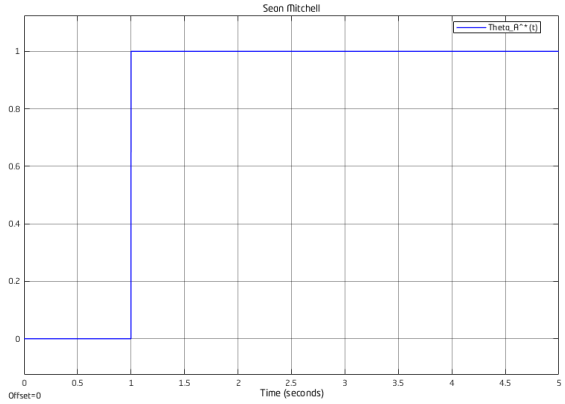

Figure 6: Simulation of $\theta_a^*(t)$ (rad) vs time (s)

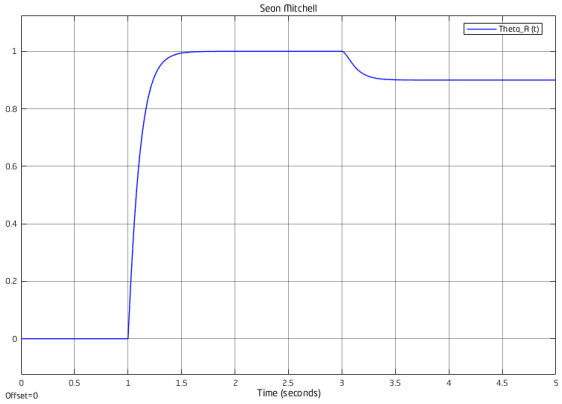

Figure 7: Simulation of $\theta_a(t)$ (rad) vs time (s)

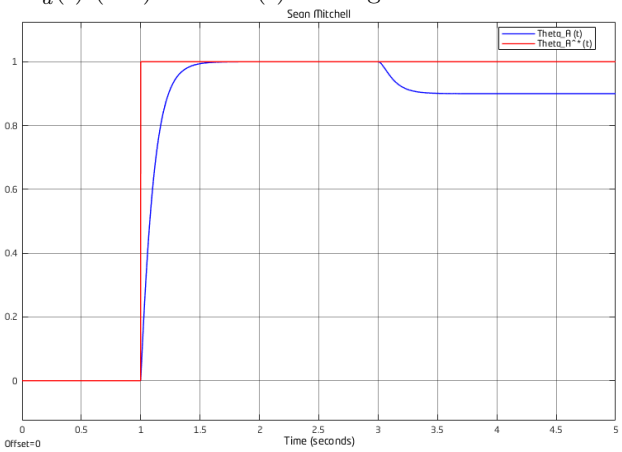

Figure 8: Simulation of $\theta_a(t)$ (rad) and $\theta_a^*(t)$ (rad) vs time (s)

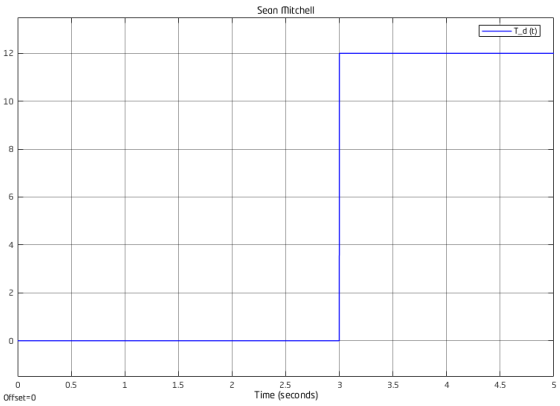

Figure 9: Simulation of $T_d(t)$ (N-m) vs time (s)

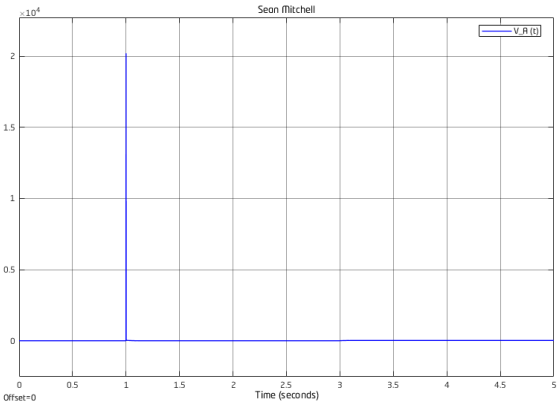

Figure 10: Simulation of $V_a(t)$ (V) vs time (s)

4.2 Simulation of PD Controller with Prefilter

The following five plots show the simulation of the PD controller with a prefilter. From these plots, it is clear the PD controller is able to successfully stabilize the angular position, θ_A, after the disturbance occurs, but the controller is not able to return it to the desired value.

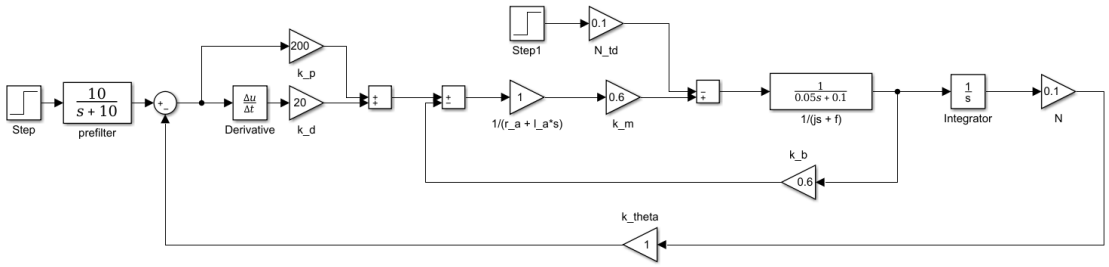

Figure 11: Block diagram of the PD controller with a prefilter

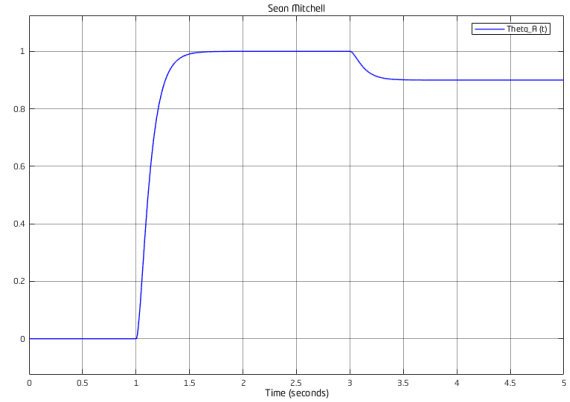

Figure 12: Simulation of $\theta_a^*(t)$ (rad) vs time (s)

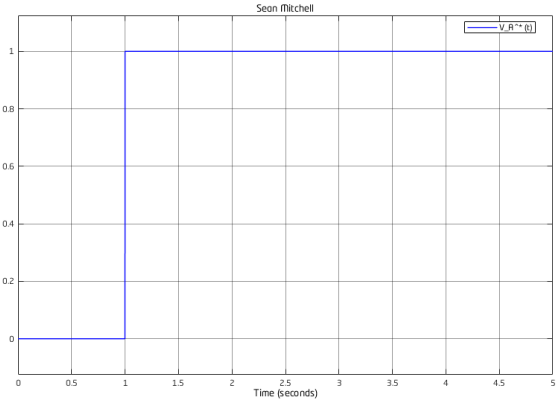

Figure 13: Simulation of $\theta_a(t)$ (rad) vs time (s)

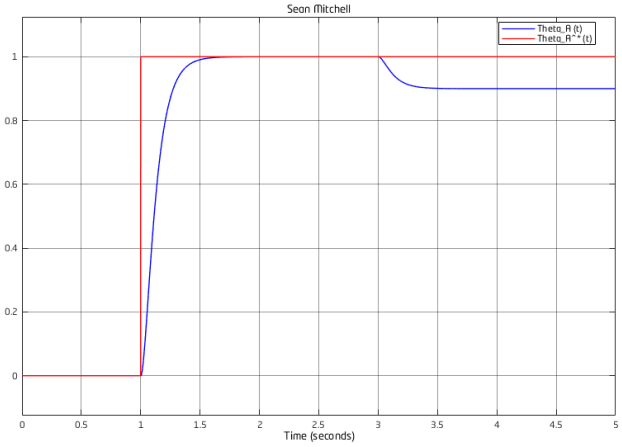

Figure 14: Simulation of $\theta_a(t)$ (rad) and $\theta_a^*(t)$ (rad) vs time (s)

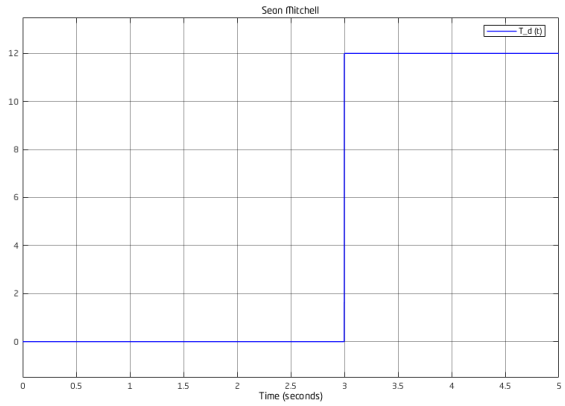

Figure 15: Simulation of $T_d(t)$ (N-m) vs time (s)

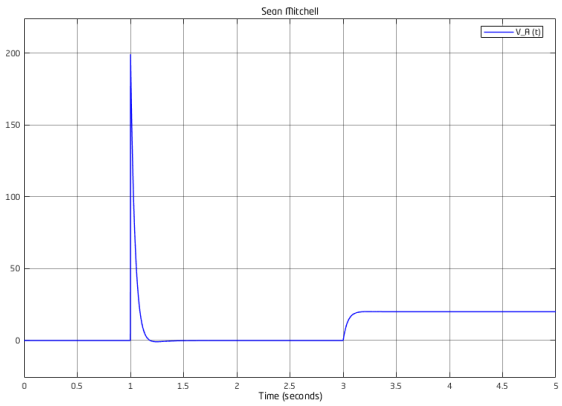

Figure 16: Simulation of $V_a(t)$ (V) vs time (s)

4.3 Simulation of PID Controller

The following four plots show the simulation of the PID controller without a prefilter. From these plots, it is clear the PID controller is able to successfully drive the angular position, θ_A, to the desired value. Once the wind disturbance is introduced, the PID controller not only keeps γ stable, but drives θ_A back to the desired value.

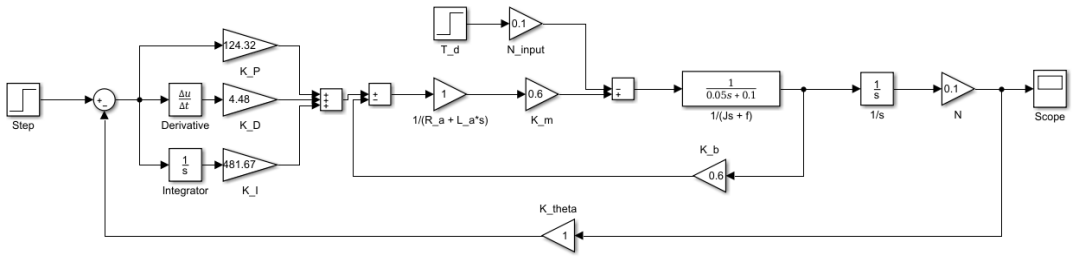

Figure 17: Block diagram of the PID controller

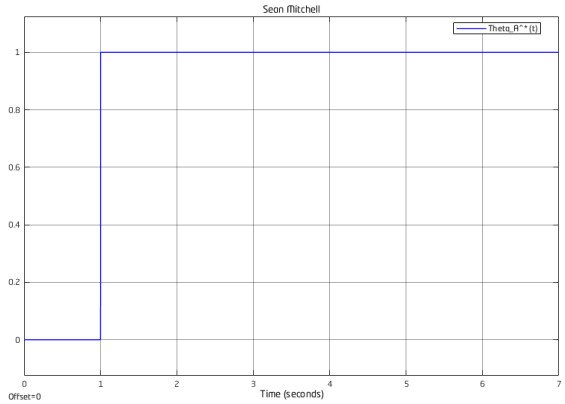

Figure 18: Simulation of $\theta_a^*(t)$ (rad) vs time (s)

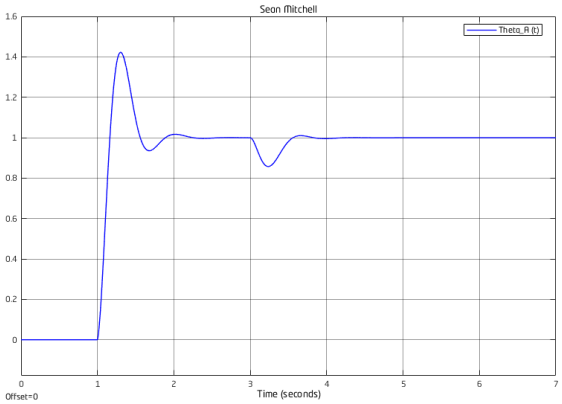

Figure 19: Simulation of $\theta_a(t)$ (rad) vs time (s)

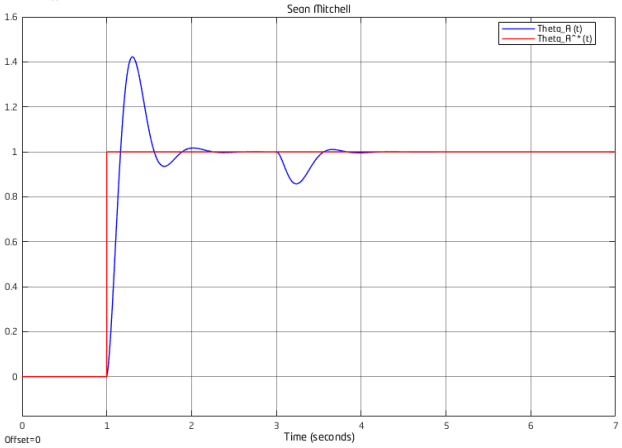

Figure 20: Simulation of $\theta_a(t)$ (rad) and $\theta_a^*(t)$ (rad) vs time (s)

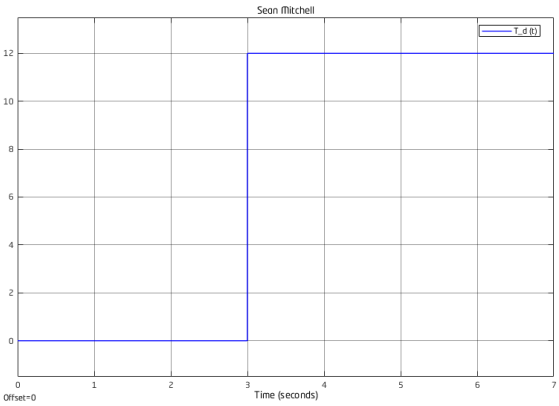

Figure 21: Simulation of $T_d(t)$ (N-m) vs time (s)

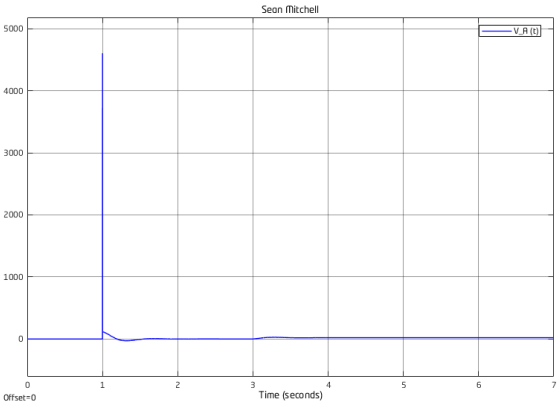

Figure 22: Simulation of $V_a(t)$ (V) vs time (s)

4.4 Simulation of PID Controller with Prefilter

The following four plots show the simulation of the PID controller with a prefilter. From these plots, it is clear the PID controller is able to successfully drive the angular position, θ_A, to the desired value. Once the wind disturbance is introduced, the PID controller not only keeps γ stable, but drives θ_A back to the desired value.

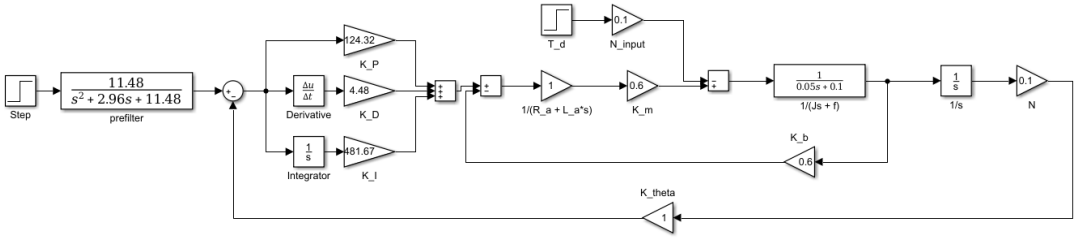

Figure 23: Block diagram of the PID controller with a prefilter

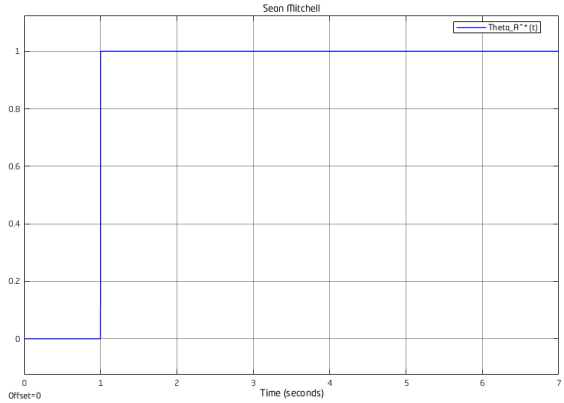

Figure 24: Simulation of $\theta_a^*(t)$ (rad) vs time (s)

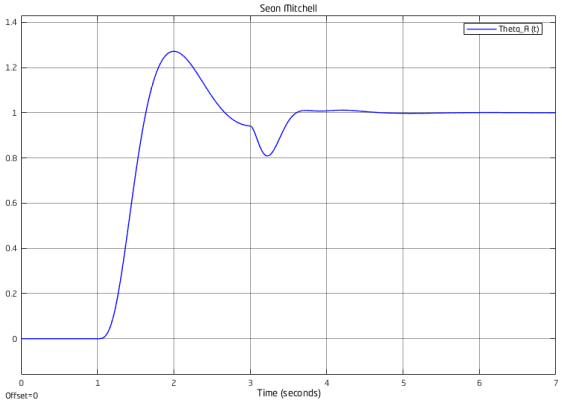

Figure 25: Simulation of $\theta_a(t)$ (rad) vs time (s)

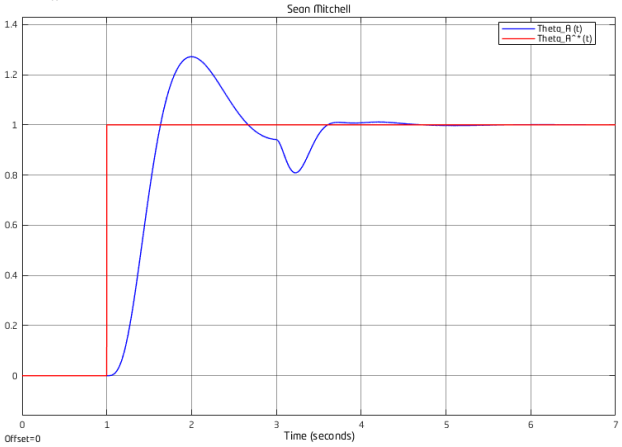

Figure 26: Simulation of $\theta_a(t)$ (rad) and $\theta_a^*(t)$ (rad) vs time (s)

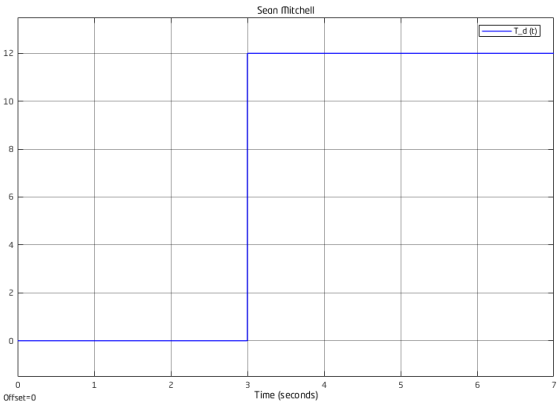

Figure 27: Simulation of $T_d(t)$ (N-m) vs time (s)

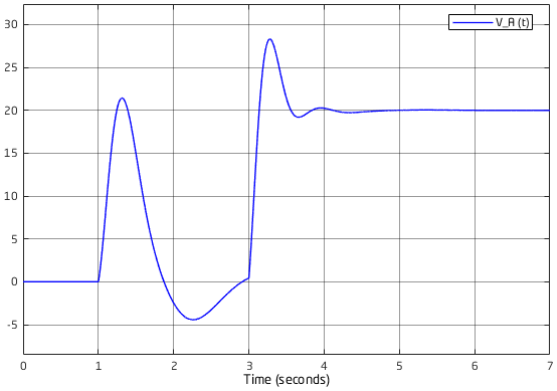

Figure 28: Simulation of $V_a(t)$ (V) vs time (s)

5 Conclusion

In conclusion, the goal of this project was to derive a way to stabilize the angular position of an antenna. This goal was accomplished using two different controllers. The first controller designed was a PD controller. This controller stabilized the antenna's angular position until a disturbance was introduced. When a wind disturbance was introduced, the PD controller was unable to drive the antenna's angular position back to the desired value. Next, a PID controller was successfully designed to set the antenna's angular position back to the desired value after a wind disturbance had been introduced. Both the PD and PID controller were designed and simulated with and without a prefilter.

Comparing the results of the four control systems, the PD controllers were only useful in this scenario if there was no disturbance. Between the two PD controllers, the pd controller with a prefilter was more efficient when comparing the voltage plots. Both the PID controllers were able to successfully stabilize and drive the antenna's angular position back to the desired value after a disturbance occurred. Between the two PID controllers, the PID controller with a prefilter was more efficient when comparing the voltage plots. However, comparing the output plots, the PID controller with a prefilter takes longer to reach steady state than the PID controller without a prefilter.

All four control systems were capable of driving the antenna's angular position to a given input, but only the PID controllers could handle a disturbance. However, this additional level of control is harder to achieve. The PID controller is more complicated to design and build when compared to the PD controller.

6 Appendix

6.1 References

[1] R. Dorf and R. Bishop, Modern Control Systems. Boston, MA: Pearson, 2016, pp. 319.